Science of the Total Environment 751 (2021) 142292

Contents lists available at ScienceDirect

Science of the Total Environment

journal homepage: www.elsevier.com/locate/scitotenv

Using easy-to-biodegrade co-substrate to eliminate microcystin toxic on electrochemically active bacteria and enhance bioelectricity generation from cyanobacteria biomass

Fabrice Ndayisenga [a,b], Zhisheng Yu [a], Ge Yan [b], Irfan Ali Phulpoto [a], Qingcheng Li [b,c], Haresh Kumar [b], Liang Fu [b], Dandan Zhou [b,*]

[a] College of Resources and Environment, University of Chinese Academy of Sciences, Beijing 100049, China
[b] Engineering Lab for Water Pollution Control and Resources Recovery of Jilin Province, School of Environment, Northeast Normal University, Changchun 130117, China
[c] State Key Joint Laboratory of Environment Simulation and Pollution Control, School of Environment, Tsinghua University, Beijing 100084, PR China

HIGHLIGHTS

- Toxic cyanobacteria converted to electricity via EAB with aid of co-substrate.
- Co-substrate enhanced energy recovery from cyanobacteria biomass via an MFC.
- Co-substrate increased MC-LR removal efficiency by 64.7% and so eliminated the toxins in the analyte.
- Co-substrate promoted MC-LR degrading bacteria and EAB cell enrichment.
- Coulombic efficiency increased by 60.1% when the co-substrate was sufficient.

GRAPHICAL ABSTRACT

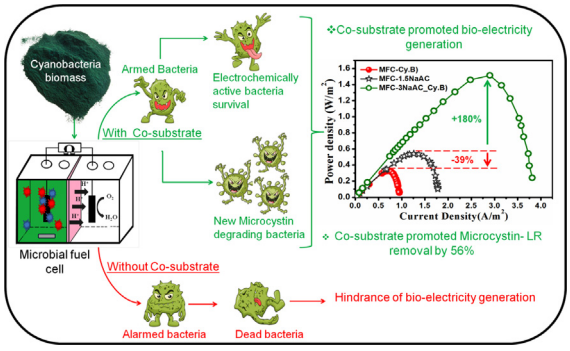

ARTICLE INFO

Article history:
Received 27 July 2020
Received in revised form 6 September 2020
Accepted 7 September 2020
Available online 12 September 2020

Editor: Huu Hao Ngo

Keywords:
Microcystis aeruginosa biomass
Bio-energy production
Microbial fuel cell
Microcystin-LR degrading bacteria
Toxic cyanobacterial bloom

ABSTRACT

Cyanobacterial biomass is a promising natural resource for power generation, through the reactions bio-catalyzed by electrochemically active bacteria (EAB). However, the major limitation is the involvement of Microcystin-LR (MC-LR) in inhibiting EAB activation. In this work, toxic *M. aeruginosa* biomass was employed as analyte of a microbial fuel cell (MFC), and sodium acetate was applied as easy-to-biodegrade co-substrate to alleviate the MC-LR stress on EAB survival. The running stability was continuously enhanced with the increment of co-substrate concentration. The sufficient co-substrate supply (6.0 mM) eliminated the negative effects of MC-LR on the cyanobacteria biomass fed-MFC performance; it contributed 12.7% extension on the electric cyclic terms and caused the productions of the power density which was comparable and even 3.8% higher than its corresponding control (MFC treated with acetate alone). The co-substrate addition also increased coulombic efficiency by 60.1%, microcystin-LR removal efficiency increased by 64.7%, and diversified the microbial community with more species able to biodegrade the MC-LR, bio-transforming the metabolites and EAB. Microcystin-degrading bacteria, such as *Sphingopyxis sp.*, *Burkholderia-Paraburkholderia*, and *Bacillus sp.*, were remarkably increased, and EAB, including *Shewanella sp.*, *Desulfovibrio desulfuricans*, *Aeromonas hydrophila*, were also much more enriched in co-substrate use protocol. Therefore, this study verified a co-substrate strategy for simultaneously eliminating MC-LR toxin and enhancing bioelectricity generation from cyanobacterial biomass via an MFC.

* Corresponding author.
E-mail address: zhoudandan415@163.com (D. Zhou).

https://doi.org/10.1016/j.scitotenv.2020.142292
0048-9697/

1. Introduction

The harmful cyanobacteria blooms are a major global problem affecting the aquatic ecosystems (Kruger et al., 2012). What is more, cyanobacteria commonly produce a kind of potent toxin, Microcystin-LR (MC-LR), which primarily affects the hepatocytes and inhibits the protein phosphatases and prevents the formation of the cytoskeleton (Fromme et al., 2000; Schmidt et al., 2014). This could result in fostering oxidative stress in liver tissues and then kill the aquatic life (Smith et al., 2008). Constructive measures to control the existence of cyanobacteria biomass and eradicate their toxic metabolites should eagerly be taken.

Nevertheless, cyanobacteria contribute to the reduction of greenhouse gases in the aquifer as they use CO_2 for chemoautotrophy growth, and are also widely used in food industries and other biotechnological applications because they are enriched of a high amount of nutrients such as proteins, carbohydrates, vitamins, and lipids. This implied that the cyanobacteria biomass could also be regarded as bio-resources for generating renewable and sustainable energy (Rastogi and Sinha, 2009). In this context, the collected cyanobacterial biomass from the eutrophicated lakes could be a promising sustainable bio-analyte for power generation by employing microbial fuel cells (MFCs), which can use bacterial consortia and produce electricity from organic wastes (Cha et al., 2010). Thus, cyanobacterial biomass is a potential resource for power generation, through the reactions bio-catalyzed by electrochemically active bacteria (EAB), rather than bio-wastes.

However, the negative effects of toxins released by cyanobacterial biomass should be especially concerned. MC-LR could damage the bacterial cell wall, and then cross the cytoplasmic membrane to invade the central components of the bacteria cells (Fischer et al., 2005). It seems the major limitations of using cyanobacteria as bio-analyte of an MFC are the involvement of MC-LR in inhibiting EAB activation and consequently decreasing the electricity transformation from cyanobacterial biomass via EAB.

It is hypothesized that the easy-to-biodegrade co-substrate could relieve the MC-LR stress on EAB and enhance the power output: fostering robust biofilm formation to resist to the recalcitrant toxin (MC-LR) and improving microbial metabolic activities (Yu et al., 2019), which led to the massive electron liberations from both toxic biomass and co-substrate. The application of co-substrate speeds up bio-oxidation reactions and stimulates the functional enzymes which result in enhancing the breakdown of the recalcitrant toxic compounds (Huang et al., 2012; Zhang et al., 2020). Moreover, a co-substrate as an additional carbon source fosters anodic bacterial growth of EAB, Microcystin-degrading bacteria, and other fermentative bacteria by supplying extra-energy (Xiong et al., 2018). Therefore, the application of co-substrate could theoretically enhance power production and toxin degradation, however, this hypothesis has not been tested yet.

A few studies have been done on exploring the electricity generation from algal biomass by using chemical catalysts, such as Pt, Pd, MnO_2, and TiO_2, to accelerate the electrochemical reactions (Bhowmick et al., 2019; Das et al., 2020; Logan et al., 2006), which were not cost-effective and the recover efficiencies were very low. Yong et al. reported the bioelectricity generation from blue-green algae biomass using MnO_2 as a catalyst, however, a maximum power density of 0.114 W/m^2 (Yuan et al., 2011) was obtained. Reimers et al. used marine plankton as electron donors of EAB, the maximum power density was only 0.017 W/m^2 (Reimers et al., 2007). The feasibility of biodegrading microcystin through biological approaches and directly produce bioelectricity from toxic cyanobacteria biomass waste in MFC have been not previously reported.

This work aims to convert toxic cyanobacteria (*M. aeruginosa*) biomass wastes to electricity through electrochemically active bacteria groups, and considerable bioelectricity generation and toxic elimination were expected. Sodium Acetate (NaAC) was employed as a model co-substrate as it is readily consumed by bacteria and is the most simple carbon source to enter the tricarboxylic acid cycle (TCA cycle) (Chae et al., 2009), and is confirmed to be an ideal electron donor for EAB (Speers and Reguera, 2012).

The toxics of hepatotoxic MC-LR on EAB were especially concerned and the contribution of NaAC on the EAB recovery was elaborated. The biochemical compositions of *M. aeruginosa* were primarily investigated to determine whether it was suitable to be used as the analyte. Then, the effects of co-substrate on the MC-LR elimination, electrochemical characteristics, and microbial community dynamics were identified, by comparing the protocols without co-substrate and with co-substrate. This novel technology will not only provide bioenergy generation but also make a remarkable contribution to aquatic purification by recycling the toxic bloom as bioresources.

2. Materials and methods

2.1. Cyanobacteria and culture medium

Microcystis aeruginosa seeds Kützing 1846 strain (FACHB 469) were obtained from Wuhan Institute of Hydrobiology, Chinese Academy of Sciences, China, and then refreshed in the modified BG11 medium (Logan et al., 2006), which was consisted of the solid ingredients and 1 mL of trace elemental solution (Luengo et al., 2014) as shown in Table 1. Refreshed cyanobacteria cells were grown in the autotrophic condition in an incubator (BLB10-5GJ-2-H, Shanghai Bailun Bio-Technology Co., Ltd., China) with an orbital shaker set at 150 rpm and the constant temperature was set at 27 ± 1 °C. The harvested cyanobacteria biomass was used as a sole carbon source for EAB growth after being pre-treated, thus its biomass powder was no longer alive in the MFC.

2.2. M. aeruginosa biomass preparation for analytes

After ~30 days of culture, the cells were collected via centrifugation (TGL-16M, CENCE, China) at 10,610 ×*g* for 10 min. After throwing away the supernatant, sodium chloride 0.9% was used to wash the precipitate three times and then freeze-dried. The dried pellet was first ground and then sonicated in purified water to undergo a cell lysis process using a homogenizer instrument (Scientz JY96-11N, Ningbo Scientz Biotechnology Co., Ltd., China) at 90% power for 10 min, followed by the heating process at 98 °C for 2 h in a water bath (Ndayisenga et al., 2018). This treatment method resulted in liberating intracellular compounds of cyanobacteria cells into the medium, and the solution was then filtrated by a 0.45 μm membrane (Whatman, GF/C, USA) and then ready for use as analyte. The details of the procedure of getting a pure homogenous bio-analyte are given in Fig. 1.

Table 1
Modified BG11 medium composition.

	Chemicals	Quantity mg L^{-1}
Ingredients	$NaNO_3$	1500
	$K_2HPO_4.3H_2O$	40
	$MgSO_47H_2O$	75
	$CaCl_2.2H_2O$	36
	Na_2CO_3	20
	Citric acid	6
	$FeCl_3.6H_2O$	3.15
Trace elementals (1 mL L^{-1})	$Na_2MoO_4.2H_2O$	0.39
	H_3BO_3	2.86
	$Co(NO_3)_2.6H_2O$	0.08
	$MnCl_2.4H_2O$	0.05
	$CuSO_4.5H_2O$	1.81
	$ZnSO_4.7H_2O$	0.22
	Concentrated H_2SO_4 (98%)	1 mL

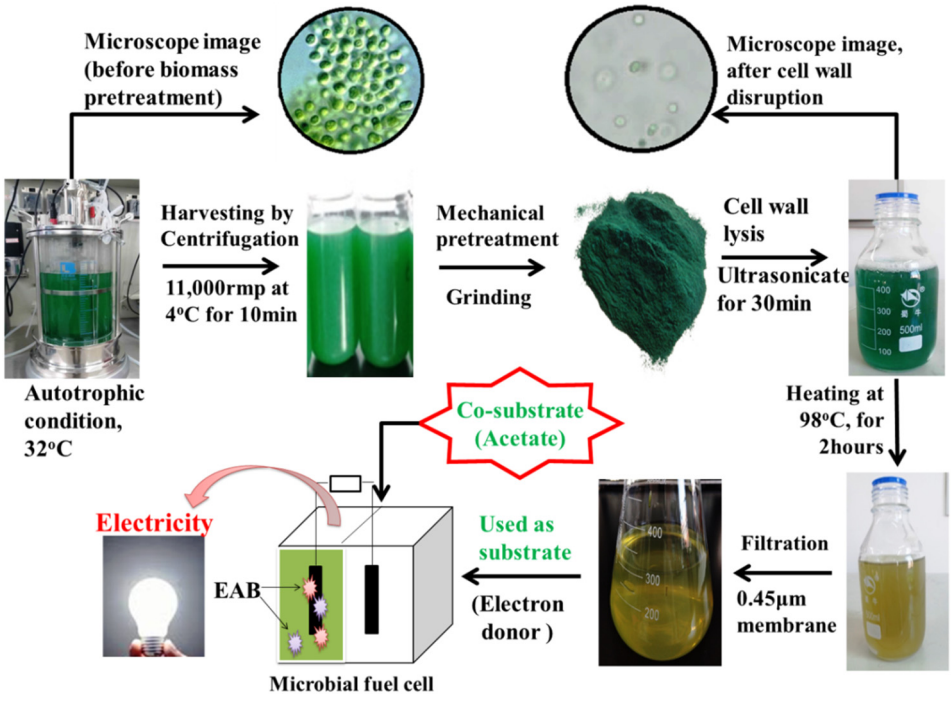

Fig. 1. Pre-treatment process of cyanobacteria biomass.

2.3. MFC construction, start-up, and operation

2.3.1. MFC construction

MFC reactor consisted of a cathode and anode chambers, each of 50 mL working volumes separated by a cation exchange membrane (Ultrex CMI – 7000, Membrane International, USA) was constructed. Carbon felt (9 cm^2) and carbon cloth (9 cm^2) were employed as anode and cathode electrode respectively; connected via copper wire and a fixed resistor of 1000 Ω (Fig. S1).

2.3.2. MFC start-up and operation

Anaerobic sludge (10% v/v) collected from a municipal wastewater treatment plant was inoculated into the anode chamber as EAB seeds. The anodic medium and cathodic solution at the start-up term was set as previously reported by Logan et al. (Logan et al., 2006). In the acclimatization period, the NaAC (10 mM) served as a source of carbon and electron donor, and pH was set to 7.2 at initial according to Patil et al. (2016) and Pham et al. (2006). MFC was running at a temperature-controlled room (25 ± 1 °C).

Pre-treated cyanobacteria biomass analyte was applied in the anodic chamber of the MFC when the electric batch cycle stayed stable; the sodium acetate as co-substrate was added when necessary, as shown in Table 2. The anolyte was replaced when the voltage output became below 50 mV.

Table 2
Composition of anolyte and catholyte in the MFC.

Protocols	Anolyte			Catholyte	
	Biomass (mg/L-COD)	Co-substrate (NaAC) (mM)	PBS (mM)	$K_3[Fe(CN)_6]$ (mM)	PBS (mM)
1.5AC	/	1.5	50	100	50
1.5AC + CYB	200	1.5	50	100	50
3.0AC	/	3.0	50	100	50
3.0AC + CYB	200	3.0	50	100	50
6.0AC	/	6.0	50	100	50
6.0AC + CYB	200	6.0	50	100	50
CYB	200	/	50	100	50

2.4. Analytical methods

2.4.1. Chemical analysis

Biological oxygen demand (BOD_5) was evaluated as described by Lenore et al. (Lenore S. Clesceri et al., 2005) and the test was conducted for 5 days. Chemical oxygen demand (COD) was determined according to the standard methods 5220 as previously reported by APHA et al. (1999), and it helped to investigate the biodegradability of cyanobacterial biomass based on BOD_5/COD (Choi et al., 2017; Kreetachat et al., 2007). Total protein was measured following Lowry protein assays as previously reported by Choi et al. (2016), and Carbohydrate concentrations were quantified based on anthrone reagent as previously described (Turula et al., 2010). Lipid content was measured using chloroform-methanol reagent as described by Fu et al. (2019) and the toxin (Microcystin-LR) was quantified using enzyme-linked immunosorbent assay (ELISA) kit (Jianglai Biological Technology, Shanghai, China) equipped with a UV detector (Chen et al., 2004).

2.4.2. Electrochemical analysis

The MFC cell potentials across a resistor were recorded every 3 min using a multimeter (Model 2700, KeithleyInstru. USA). Current (I) was obtained based on Ohms law, I = U/R where U stands for the recorded voltage and R for a fixed resistance. Current density (J) was obtained using the equation: I/A, where A represents the working surface area of the anode and power density (P) was obtained using the equation: U. J. Coulombic efficiencies (CEs) were calculated as previously reported by Gadkari et al. (2019) and Cyclic voltammetry (CV) was obtained as described by Yu et al. (2019).

2.4.3. Statistical analysis methods

Basic descriptive statistics, data treatment, figure drawings, and locating the oxidation and reductions peaks for CV curves were all done using ORIGIN software _v9.sr2 and Microsoft Excel. *t*-Test was employed to determine whether the power density decrement and increment caused by MC-LR and co-substrate respectively are statistically different at $p < 0.05$ level of significance.

2.5. Electron microscopy observations

The microbial ultra-structure observation was made possible via transmission electron microscopy (TEM; JEM1200, JEOL Ltd., Japan) and sample pre-treatment methods are provided in Text S2.

2.6. Microbial community analysis

Microbial samples were collected from the anode chamber by placing a small section of anode electrode in centrifuge tubes containing sterile 0.02 M PBS solution, and then vortexed for the 30s. Fibers were removed and the remaining content was centrifuged at 5000 ×g, for 7 min. The supernatant was discarded and the pellet was kept for microbial community analysis performed as described by Cui et al. (2018). The extraction of the DNA was performed following the Fast DNA Spin Kit for Soil protocol (E.Z.N.A. Soil DNA Kit, Omega, USA) and the amplification of the bacterial 16SrRNA V3-V4 fragments occurred on F338 (ACTCCTACGGGAGGCAGCAG) and R806 (GGACTACHVGGGTWTCTAAT) primers (Cui et al., 2018).

3. Results and discussion

3.1. Potentialities and challenges of cyanobacteria as the electron donor

M. aeruginosa biomass is mainly composed of protein 0.57 g/g, lipid 0.31 g/g, and carbohydrates 0.08 g/g (in dry weight biomass, DW) (Fig. S3). They were approximately 96% of the total biomass; the left part could be cell-wall debris and other trace intercellular components. The high biodegradability of *M. aeruginosa*, represented by BOD_5/COD, was ~0.65, which revealed a great potentiality of cyanobacterial biomass as the electron donors for electricity generation. The biochemical composition findings in this study were comparable to the previous reports (Khan et al., 2016).

However, the big challenge for using cyanobacterial biomass as analytes was the intracellular toxins (MC-LR), which were inevitably included in the biomass slurries (Oh et al., 2000). The detected MC-LR in *M. aeruginosa* biomass was 44.14 μg/g-DW, and such level in the anolyte could virtually inhibit the EAB growth (Bury et al., 1995; Fischer et al., 2005). The MFC treated with *M. aeruginosa* biomass slurry free of co-substrate (MFC-CYB), attributed a very low power density output of 43 mW/m^2 at the first cycle. Then, the electric cycle time justified by power density output, values dropped more and more dramatically during the long term running (Fig. S5). This indicated the inactivity of EAB caused by the above-mentioned high MC-LR level. Therefore, a new strategy should be adopted to alleviate the toxicity of the MC-LR on bacterial growth.

3.2. Roles of co-substrate in electricity generation

3.2.1. Enhanced running stability

Co-substrate strategy was employed to improve EAB survival and electron liberation capability. The findings showed that the reactors treated with insufficient co-substrate supply, the MC-LR caused noticeable inhibition of power output, thus resulted in shortening at certain extends comparing to their parallel reactors treated with acetate alone (control) (Fig. 2a). However, the more we augmented the co-substrate concentration, the more the MC-LC effects to power generation was minimized (Fig. 2). For example, when the co-substrate was 1.5 mM and 3 mM, the toxins of cyanobacteria biomass caused the maximum power density to dramatically decrease by 8.88% and 5.01% compared to their corresponding systems treated with acetate alone (controls) respectively. However, the power generated for 6.0AC + CYB was higher than that of MFC treated only with 6AC (control) even though the difference was negligible, and the calculated CE of MFC-6.0 AC + CYB significantly increased by 58.72% ($p < 0.05$). Furthermore, the electric cyclic terms for 6.0 AC + CYB were also 12.7% more extended, as compared to its parallel protocol 6.0AC (Fig. 2c).

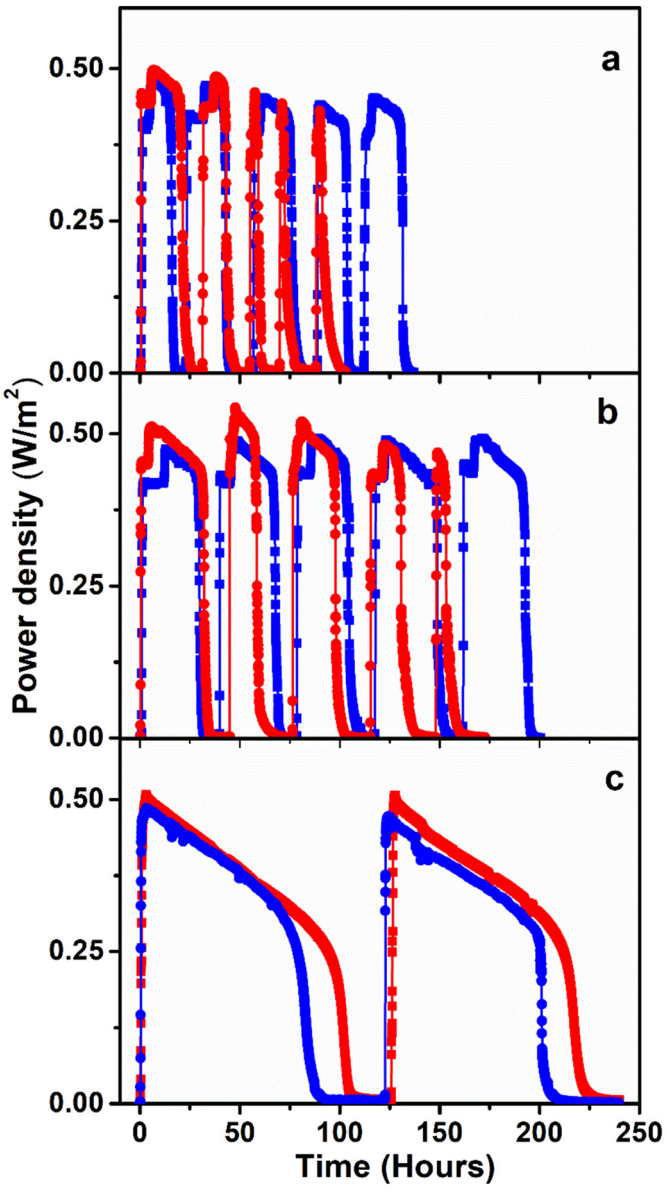

Fig. 2. Power generation of MFCs (an external resistor of 1000 Ω) using *Microcystis aeruginosa* biomass (200 mg/L-COD) as analyte, supplemented with different concentrations of co-substrate. Red color stands for biomass with co-substrate addition, whereas blue color stands for the co-substrate alone. (a) MFC-1.5AC + CYB vs. MFC-1.5AC; (b) MFC-3.0AC + CYB vs. MFC-3.0AC; (c) MFC-6.0AC + CYB vs. MFC-6.0AC. (For interpretation of the references to color in this figure legend, the reader is referred to the web version of this article.)

The *M. aeruginosa* fed MFC presented continuously enhancement on the running stability with the increment of co-substrate concentration. Moreover, the maximum power density generation was ideally increased along with the augmentation of the co-substrate concentration (Fig. 2a–c), indicating the conspicuous function of the co-substrate in enhancing the bio-electrochemical activities, detoxifying the MC-LR for anode biofilm formation (Zhang et al., 2020). Furthermore, co-substrate favored the biodegradation of complicate nutritional compounds present in the biomass to the easy-to-biodegrade substrate, to support EAB growth and utilize and transfer donated electrons (Huang et al., 2012; Xiong et al., 2018; Yu et al., 2019). These results confirmed that *M. aeruginosa* biomass successfully worked as a sole carbon source for bacterial growth.

3.2.2. Promoted power production

Based on the polarization tests, the MFC treated with co-substrate was directly compared with their parallel MFCs treated only with acetate (Fig. 3a–c). CYB alone protocol failed to have a polarization test due to the running was collapsed (Fig. S4). When the co-substrate was 1.5 mM, the toxins of cyanobacteria biomass caused the maximum power density to dramatically decrease by 32.0% compared to its parallel control (1.5-AC vs. 1.5-AC + CYB) (Fig. 3a) ($p < 0.05$). The sufficient co-substrate supply (6.0 mM) eliminated the negative effects of MC-LR on the MFC performance and caused the productions of the power density which was comparable and even 3.8% higher than its corresponding control (MFC treated with acetate alone) (Fig. 3c).

Likewise, the maximum current density also increased along with the augmentation of the co-substrate, as shown in Fig. 3d–f, which dropped 15.3% when acetate co-substrate was 1.5 mM as compared with the none CYB protocol, but increased 2.3% with 6.0 mM acetate co-substrate. Based on the combined results shown in Fig. 3, co-substrate supply enhanced the survival and activity of EAB cells which were responsible for electrons transfer from both cyanobacteria biomass and co-substrate. Thus, even the maximum power densities and current density output were less affected, and the sufficient co-substrate (6.0AC + CYB) contributed to a longer running cycle. Thus, CE represents the charge efficiency by which electrons are transferred in the MFCs, significantly increased from 8.93% for 1.5AC + CYB to 67.7% for 6.0AC + CYB protocol ($p < 0.05$) and compared to MFC treated with acetate alone, the co-substrate addition protocol remarkably increased coulombic efficiency by 60.1% ($p < 0.05$) which attributed to the elimination of the toxics in cyanobacterial biomass on EAB.

Fig. 4 conspicuously revealed that cyanobacteria, probably MC-LR toxin, caused notable damaging on both the cell wall (CW) and plasma membrane (PM) (Fig. 4a), which diminished the EAB metabolic activities and thus provoked the less electric power; this was consistent with Miguens et al's report (Miguéns and Valério, 2015). Microcystin can permeate into the intracellular of the bacterial cell (Dixon et al., 2004), by pervading the outer membrane (cell wall) and then cross the plasma membrane through organic anion polypeptide transporters (Fischer et al., 2005). In contrast, with sufficient co-substrate (6.0AC + CYB), the bacterial cell morphology was less affected by the toxin (Fig. 4b). Therefore, the co-substrate strategy could relieve MC-LR stress on bacterial growth; these were consistent with the high output power produced in the co-substrate-used protocol.

3.2.3. Altered cyclic voltammetry (CV) curves

The electrochemical behaviors characterized by CV curves are clearly described in Fig. 5. The co-substrate free protocols showed only the oxidation peak at the potential of −0.175 V and the reduction peak

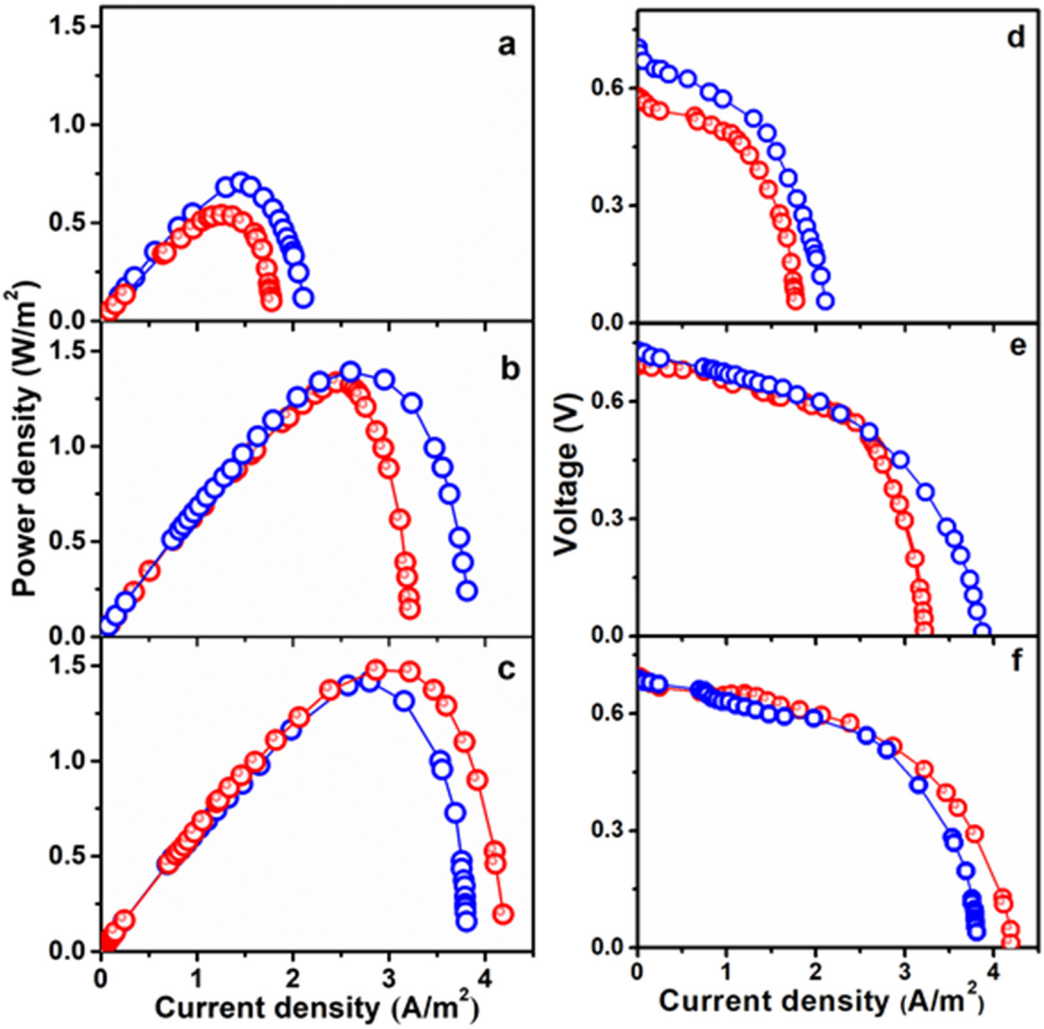

Fig. 3. Representative power density (a, b, c) and polarization (d, e, f) curves for MFCs treated with different concentrations of co-substrate during *Microcystis aeruginosa* biomass (200 mg/L-COD) degradation, equipped with an external resistor of 1000 Ω. The results were directly compared to corresponding acetate-fed MFCs. Red color stands for biomass with co-substrate addition, whereas blue color stands for the acetate alone. (a) 1.5AC + CYB vs. 1.5AC; (b) 3.0AC + CYB vs. 3.0AC; (c) 6.0AC + CYB vs. 6.0AC. (For interpretation of the references to color in this figure legend, the reader is referred to the web version of this article.)

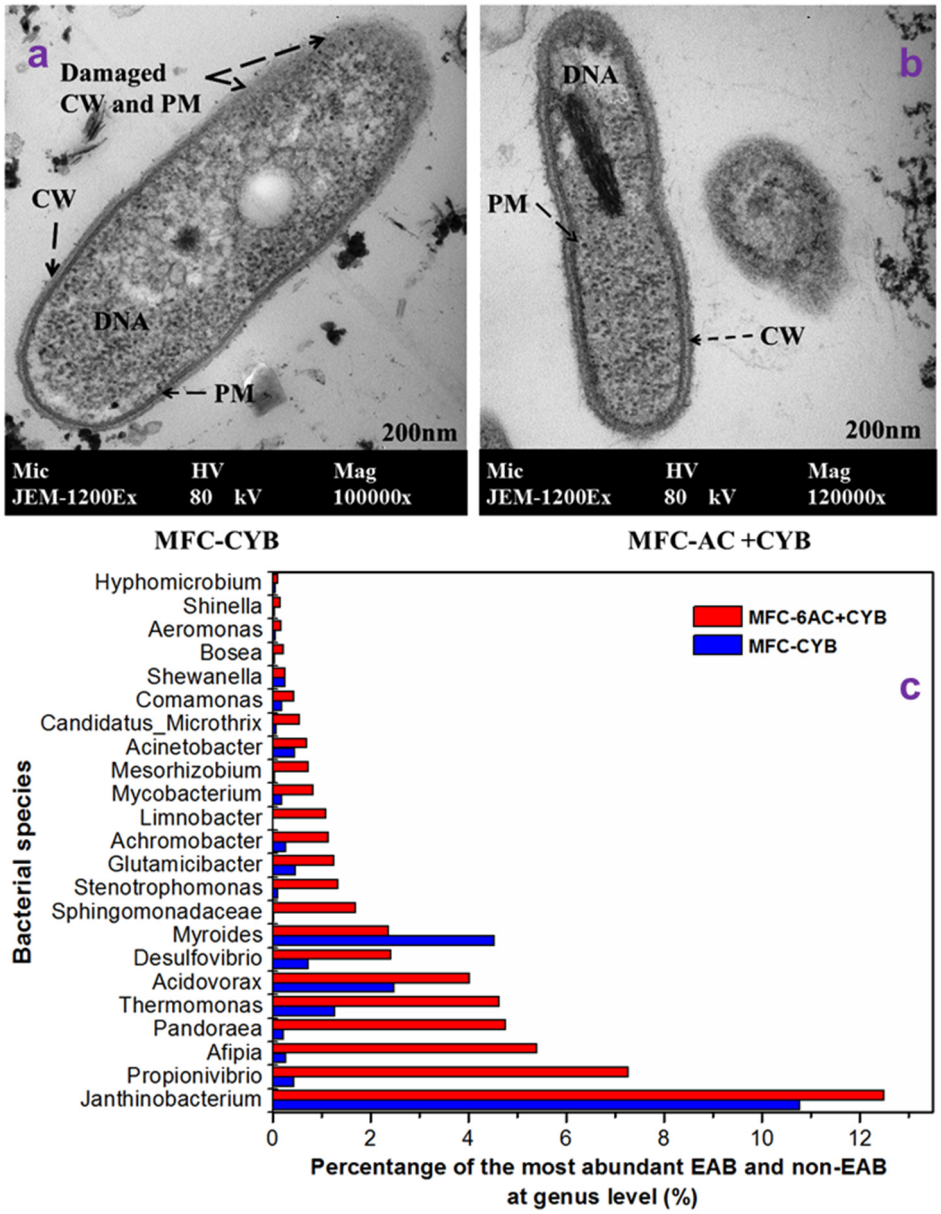

Fig. 4. Transmission electron microscopic (TEM) images of anode-bacterial cells for without co-substrate (MFC-CYB) (a) and with co-substrate addition protocol (MFC-AC + CYB) (b) respectively. PM stands for plasma membrane and CW represents the cell wall. Dominant EAB and non-EAB colonized the anodic biofilm (%) (c).

appeared at −0.556 V (vs. Ag/AgCl) (Fig. S5). Whilst, the protocols with co-substrate supplying, displayed two oxidation peaks at more positive potentials, centered at ~+0.090–0.190 V and ~−0.330 V (vs. Ag/AgCl) (Fig. 5). The appearance of two oxidation peaks in this protocol indicating the bio-anode was cloned by a more diverse bacterial community, with different pathways of transferring electron charges to the anode (Zhu et al., 2012).

These oxidation peaks were of course caused by consortia of diverse bacteria, with variable electron transfer pathways. For example, pyrroloquinoline quinone (PQQ) mediator (Freguia et al., 2010) has electrochemically driven activities that centered at +0.141 V, which is closer to the oxidation peak found at +0.090–0.190 V. In addition, the peak displayed at low potential (~−0.3 V vs. Ag/AgCl) was also probably caused by phenazine-1 carboxylic acid as electron shuttle at the mid-point potential of −0.323 V (vs. Ag/AgCl) (Bellin et al., 2014). *Shewanella* sp. and *Mycobacterium sp*., which represented ~0.3% and ~0.8% of the total anodic bacterial population respectively (see Fig. 4), could also be the cause of that peak due to tetraheme flavocytochrome *c* fumarate reductase; a 63.8-kDa soluble protein secrete by them and it's known to assist the electron transfer to bio-anode. It drives the electrochemical activities in the dynamic range of −0.32 V to −0.24 V (Bhaskar et al., 2014).

The other noteworthy point is that all co-substrate use protocols showed the oxidation peaks with higher oxidation current than those of the paralleled acetate alone (Fig. 5a–c). Again, the results verified the contribution of cyanobacterial biomass on power generation.

3.3. Microbial community characterization

3.3.1. Dominant electrochemically active bacteria (EAB)

The use of co-substrate in the cyanobacteria biomass biodegradation has notably changed the microbial consortia composition (Fig. 6). Compared to the co-substrate free protocol, the abundance

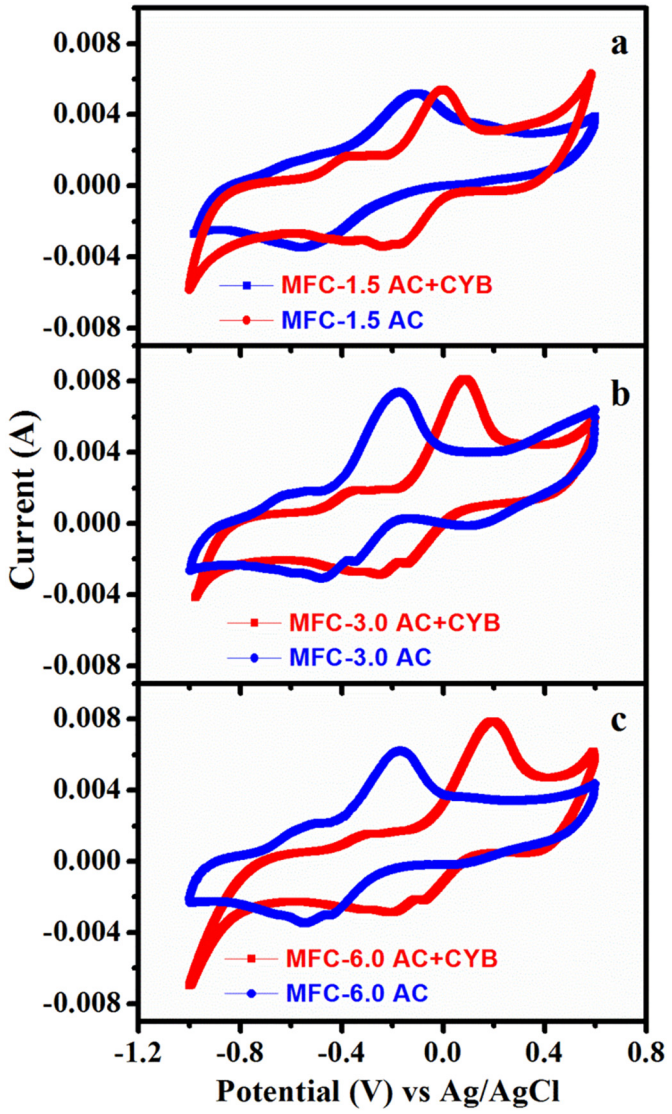

Fig. 5. Cyclic voltammetry curves of the MFCs bio-anode operated under different concentration of co-substrate during bio-oxidation of *Microcystis aeruginosa* biomass (200 mg/L-COD) for electricity production. The results were directly compared to corresponding acetate-fed MFCs.

of the well known EAB to produce substantial bioelectricity, such as *Desulfovibrio desulfuricans*, *Aeromonas hydrophila*, *Stenotrophomonas sp.*, *Mycobacterium sp.*, *Acinetobacter* sp. and *Comamonas sp.* (Bhaskar et al., 2014; Cao et al., 2019; Freguia et al., 2010; Venkidusamy and Megharaj, 2016), dramatically increased by 57%–1253% for 6AC + CYB (Fig. 4c).

Additionally, the non-EAB genera e.g., *Pandoraea sp.*, *Afipia sp.*, *Mesorhizobium sp.*, *Propionivibrio sp.*, and *Candidatus microthrix* increased by 654–2059% in the anodic biofilm of 6AC + CYB (Fig. 4c). These non-EAB were reported in converting recalcitrant complex carbon compounds into simple molecules and scavenging oxygen for electricity generation (Jung and Regan, 2007; Ndayisenga et al., 2018).

Furthermore, several new bacterial species belonged to both EAB and non-EAB appeared; Table 3 gives some typical ones. These new species also played an important role either in breaking down both toxin and other recalcitrant compounds or facilitating electrons transfer to bio-anode. For example, *Rhizobium sp.*, *Hyphomicrobium sp.*, *Brevibacterium sp.*, *Sphingomonas sp.*, abundantly appeared in the MFC-AC + CYB biofilm, were reported to completely degrade MC-LR (Briand et al., 2016; Dziga et al., 2013; Massey and Yang, 2020; Tsao et al., 2017). *Comamonas testosteroni* and *Nocardia* sp. showed the ability to degrade complex organic compounds including cyanobacterial toxins (Berg et al., 2009; Wu et al., 2015). *Delta_proteobacterium-Phaselicystis* and Bacteria appertaining to Sphingobacteriales order also involved in MC degradation, even though their exact role in the degradation process is still unknown (Kohler et al., 2014).

Comamonas testosteroni was also reported as EAB capable of degrading hydrocarbon in electrochemical fuel cells (Bianco et al., 2020; Kumar et al., 2016), and bacteria of *Sphingobacteriales* was commonly found as part of the anodic microbial community (Adessi et al., 2018). This indicates the considerable potentials of co-substrate (acetate) in promoting bacterial diversity and enhancing the MC-LR toxin degradation, which resulted in increasing the power density output. Co-substrate strategy could potentially suitable for enhancing power generation from other toxic hydrocarbons via microbial electrochemical technique.

3.3.2. Dominant MC-LR degrading bacteria

The results in Table 4 clearly show the attribution of co-substrate on promoting the resistant and robust anodic biofilm. The addition of acetate significantly enhanced MC-LR degrading bacteria species in the biofilm. Compared to cyanobacteria biomass fed MFC without co-substrate (CYB), *Stenotrophomosa sp.*, *Burkholderia-Paraburkholderia*, and *Bacillus sp.* (Kumar et al., 2019; Pearson et al., 2010), increased respectively by 1253%, 35%, and 15.3% when acetate co-substrate was 6.0 mM; AC-3.0-CYB presented the same trends (Table 4).

Particularly, *Sphingopyxis* sp. enhanced by as much as 1800%, enriches genes encode *mlr* enzymes that responsible for the hydrolyzation MC-LR; it could degrade MC-LR efficiently into the simple organic matter, such as amino acids, which could easily be assimilated by microbes (Imanishi et al., 2005). *Sphingopyxis* sp. could also relieve the bacterial growth threats which lead to the accelerated breakdown of cyanobacteria biomass and consequently generate high power (Dziga et al., 2013; Gagala and Mankiewicz-Boczek, 2012). The above results were consistent with the MC-LR removal gradient where AC6.0 + CYB showed a higher MC-LR removal efficiency of 56% than CYB alone (34%) within 6 days of one batch of the electric cycle.

4. Conclusion

The addition of the easily biodegradable co-substrate during toxic *Microcystis aeruginosa* biomass degradation in MFC, increased MC-LR removal by 64.7%, extended by 12.7% the electric cyclic terms, the power densities were 3.8% increased, and the CE increased by 60.1% as compared to the parallel system treated only with acetate. The co-substrate addition also promoted the microbial community by enriching more diverse species including MC-LR degrading bacteria, EAB, hydrocarbon-degrading bacteria and other species able to biotransforme the metabolites. Therefore, the toxic cyanobacterial biomass wastes collected from the eutrophicated aquatic environment is highly recommended to serve as the main carbon source in MFC for bioelectricity production and simultaneously accomplish wastewater treatment by applying sodium acetate as co-substrate. However, the use of sodium acetate is economically unviable for long-term and commercial applications. For practical engineering, real wastes that are easy-to-biodegrade and economical could be the substitute, such as food process by-products.

CRediT authorship contribution statement

Fabrice Ndayisenga: Conceptualization, Methodology, Investigation, Formal analysis, Writing - original draft. **Zhisheng Yu:** Writing - review & editing. **Ge Yan:** Resources, Software, Validation.

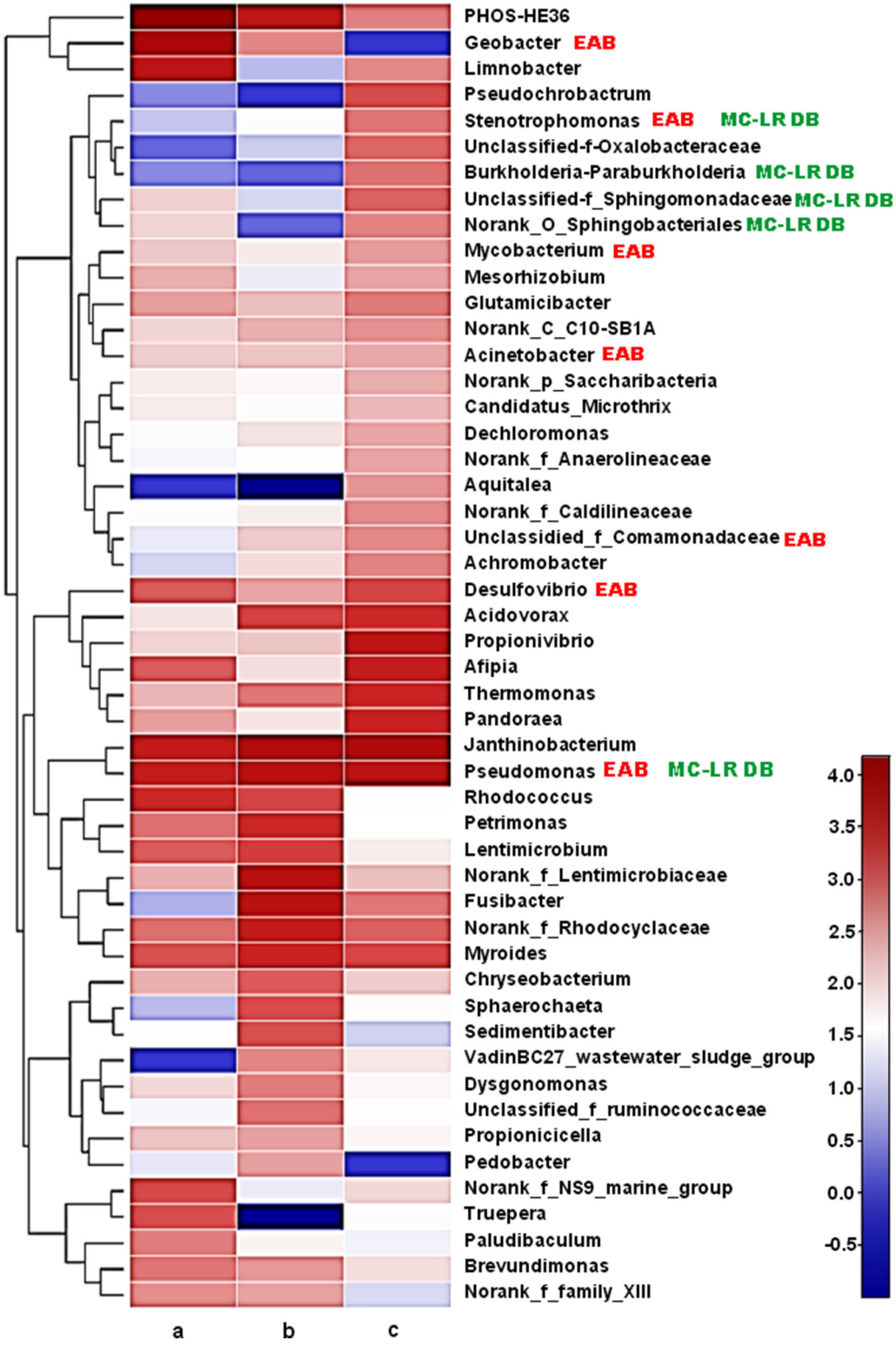

Fig. 6. Cluster analyses of microbial communities in the MFC-3AC + Cy.B (a), MFC-CYB (b) and MFC-6.0AC + CYB (c) at the genus level.

Irfan Ali Phulpoto: Writing - review & editing. **Qingcheng Li:** Resources, Software, Validation. **Haresh Kumar:** Resources, Software, Validation. **Liang Fu:** Resources, Software, Validation. **Dandan Zhou:** Conceptualization, Supervision, Funding acquisition, Project administration, Writing - review & editing.

Declaration of competing interest

The authors declare that they have no known competing financial interests or personal relationships that could have appeared to influence the work reported in this paper.

Table 3
New bacterial species appeared due to the addition of co-substrate in MFC.

No	Microbial species	Abundance in numbers		
		CYB	3.0AC + CYB	6.0AC + CYB
1	*Bacterium_YC-ZSS-LKJ199*	–	10	3
2	*Veillonellaceae (uncultured_bacterium)*	–	35	3
3	*Angustibacter (uncultured)*	–	21	6
4	*Thiobacillus_thioparus*	–	360	7
5	*Microcystis_aeruginosa*	–	32	9
6	*Anaerolineaceae_bacterium*	–	1	10
7	*Comamonas testosteroni*	–	1	10
8	*Veillonellaceae*	–	2	10
9	*Sorangium*		30	11
10	*Gallionellaceae*	–	214	11
11	*Sphingomonas (unclassified)*	–	43	12
12	*Coriobacteriaceae (unclassified)*	–	2	14
13	*Dyella (unclassified)*	–	7	14
14	*Magnetospirillum*	–	27	16
15	*Synergistaceae*	–	1	18
16	*Parvibaculum (unclassified)*	–	276	21
17	*Acetobacteraceae_bacterium*	–	17	23
18	*Nocardia_nova (unclassified)*	–	57	32
19	*Leptolinea (soil_bacterium)*	–	1	34
20	*Truepera (uncultured_bacterium)*	–	1006	34
21	*Planctomycetaceae*	–	18	46
22	*Ferrovibrio (alpha_proteobacterium)*	–	1	47
23	*Hyphomicrobiaceae (unclassified)*	–	13	54
24	*Rhizobium (unclassified)*	–	1	113
25	*Delta_proteobacterium_g__Phaselicystis*	–	58	143
26	*Aquitalea (unclassified)*		1	424
27	*Sphingobacteriales (uncultured_bacterium)*	–	157	523

Table 4
Microcystin-degrading bacteria abundance in anode biofilm promoted by co-substrate strategy (% at genus level).

Genus	CYB	3AC + CYB	6AC + CYB	References
Brevibacterium sp	0.000	0.008	0.002	(Kato et al., 2009)
Sphingopyxis sp	0.008	0.187	0.152	(Gagala and Mankiewicz-Boczek, 2012)
B. Paraburkholderia	0.004	0.006	1.405	(Kato et al., 2009)
Stenotrophomonas	0.098	0.014	1.326	(Chen et al., 2010)
Rhizobium sp	0.000	0.002	0.242	(Ramani et al., 2012)
Sphingomonas sp	0.000	0.084	0.026	(Ishii et al., 2004; Kato et al., 2009)
Bacillus sp	0.013	0.023	0.015	(Ishii et al., 2004)
Sphingomonadaceae	0.021	0.315	1.686	(Ishii et al., 2004)
Microcystis sp.	0.000	0.062	0.019	(Kormas and Lymperopoulou, 2013)

Acknowledgment

This work was supported by the National Natural Science Foundation of China (51722803); Fundamental Research Funds for the Central Universities (2412018ZD013) and the Chinese Academy of Sciences and The World Academy of Sciences (CAS-TWAS) President's Fellowship for International Ph.D. Students, for which authors are grateful.

Appendix A. Supplementary data

Supplementary data to this article can be found online at https://doi.org/10.1016/j.scitotenv.2020.142292.

References

Adessi, A., Venturi, M., Candeliere, F., Galli, V., Granchi, L., De Philippis, R., 2018. Bread wastes to energy: sequential lactic and photo-fermentation for hydrogen production. Int. J. Hydrog. Energy 43, 9569–9576.

APHA, AWWA, WEF, 1999. Standard Methods for the Examination of Water and Wastewater. APHA, AWWA, WEF, Washington, D.C.

Bellin, D.L., Sakhtah, H., Rosenstein, J.K., Levine, P.M., Thimot, J., Emmett, K., et al., 2014. Integrated circuit-based electrochemical sensor for spatially resolved detection of redox-active metabolites in biofilms. Nat. Commun. 5, 3256.

Berg, K.A., Lyra, C., Sivonen, K., Paulin, L., Suomalainen, S., Tuomi, P., et al., 2009. High diversity of cultivable heterotrophic bacteria in association with cyanobacterial water blooms. ISME J. 3, 314–325.

Bhaskar, A., Chawla, M., Mehta, M., Parikh, P., Chandra, P., Bhave, D., et al., 2014. Reengineering redox sensitive GFP to measure mycothiol redox potential of Mycobacterium tuberculosis during infection. PLoS Pathog. 10, e1003902.

Bhowmick, G.D., Chakraborty, I., Ghangrekar, M.M., Mitra, A., 2019. TiO2/activated carbon photo cathode catalyst exposed to ultraviolet radiation to enhance the efficacy of integrated microbial fuel cell-membrane bioreactor. Bioresour. Techno. Rep. 7, 100303.

Bianco, F., Monteverde, G., Race, M., Papirio, S., Esposito, G., 2020. Comparing performances, costs and energy balance of ex situ remediation processes for PAH-contaminated marine sediments. Environ. Sci. Pollut. Res. Int. 27, 19363–19374.

Briand, E., Humbert, J.F., Tambosco, K., Bormans, M., Gerwick, W.H., 2016. Role of bacteria in the production and degradation of Microcystis cyanopeptides. Microbiologyopen 5, 469–478.

Bury, N.R., Eddy, F.B., Codd, G.A., 1995. The effects of the cyanobacterium Microcystis aeruginosa, the cyanobacterial hepatotoxin microcystin-LR, and ammonia on growth rate and ionic regulation of brown trout. J. Fish Biol. 46, 1042–1054.

Cao, Y., Mu, H., Liu, W., Zhang, R., Guo, J., Xian, M., et al., 2019. Electricigens in the anode of microbial fuel cells: pure cultures versus mixed communities. Microb. Cell Factories 18, 39.

Cha, J., Choi, S., Yu, H., Kim, H., Kim, C., 2010. Directly applicable microbial fuel cells in aeration tank for wastewater treatment. Bioelectrochemistry 78, 72–79.

Chae, K.J., Choi, M.J., Lee, J.W., Kim, K.Y., Kim, I.S., 2009. Effect of different substrates on the performance, bacterial diversity, and bacterial viability in microbial fuel cells. Bioresour. Technol. 100, 3518–3525.

Chen, J., Song, L., Dai, J., Gan, N., Liu, Z., 2004. Effects of microcystins on the growth and the activity of superoxide dismutase and peroxidase of rape (Brassica napus L.) and rice (Oryza sativa L.). Toxicon 43, 393–400.

Chen, J., Hu, L.B., Zhou, W., Yan, S.H., Yang, J.D., Xue, Y.F., et al., 2010. Degradation of microcystin-LR and RR by a Stenotrophomonas sp. strain EMS isolated from Lake Taihu, China. Int. J. Mol. Sci. 11, 896–911.

Choi, Jia, Kim, Kui-Jin, Koh, Eun-Jeong, Lee, B.-Y., 2016. Altered Gelidium elegans extract-stimulated beige-like phenotype attenuates adipogenesis in 3T3-L1 cells. J. Food Nutr. Res. 4, 448–453.

Choi, Y.-Y., Baek, S.-R., Kim, J.-I., Choi, J.-W., Hur, J., Lee, T.-U., et al., 2017. Characteristics and biodegradability of wastewater organic matter in municipal wastewater treatment plants collecting domestic wastewater and industrial discharge. Water 9, 409.

Clesceri, Lenore S., Eaton, Andrew D., Rice, E.W., 2005. Standard Methods for Examination of Water & Wastewater Method 5210B. American Public Health Association, American Water Works Association, and the Water Environment Association, Washington, DC.

Cui, X., Chen, C., Sun, S., Zhou, D., Ndayisenga, F., Huo, M., et al., 2018. Acceleration of saturated porous media clogging and silicon dissolution due to low concentrations of Al (III) in the recharge of reclaimed water. Water Res. 143, 136–145.

Das, S., Chakraborty, I., Rajesh, P.P., Ghangrekar, M.M., 2020. Performance evaluation of microbial fuel cell operated with Pd or MnO2 as cathode catalyst and Chaetoceros pretreated anodic inoculum. J. Hazard. Toxic Radioact. Waste 24, 04020009.

Dixon, R.A., Al-Nazawi, M., Alderson, G., 2004. Permeabilising effects of sub-inhibitory concentrations of microcystin on the growth ofEscherichia coli. FEMS Microbiol. Lett. 230, 167–170.

Dziga, D., Wasylewski, M., Wladyka, B., Nybom, S., Meriluoto, J., 2013. Microbial degradation of microcystins. Chem. Res. Toxicol. 26, 841–852.

Fischer, W.J., Altheimer, S., Cattori, V., Meier, P.J., Dietrich, D.R., Hagenbuch, B., 2005. Organic anion transporting polypeptides expressed in liver and brain mediate uptake of microcystin. Toxicol. Appl. Pharmacol. 203, 257–263.

Freguia, S., Tsujimura, S., Kano, K., 2010. Electron transfer pathways in microbial oxygen biocathodes. Electrochim. Acta 55, 813–818.

Fromme, H., Kohler, A., Krause, R., Fuhrling, D., 2000. Occurrence of cyanobacterial toxins–microcystins and anatoxin-a–in Berlin water bodies with implications to human health and regulations. Environ. Toxicol. 15, 120–130.

Fu, L., Li, Q., Yan, G., Zhou, D., Crittenden, J.C., 2019. Hormesis effects of phosphorus on the viability of Chlorella regularis cells under nitrogen limitation. Biotechnol. Biofuels 12, 121.

Gadkari, S., Shemfe, M., Sadhukhan, J., 2019. Microbial fuel cells: a fast converging dynamic model for assessing system performance based on bioanode kinetics. Int. J. Hydrog. Energy 44, 15377–15386.

Gagala, I., Mankiewicz-Boczek, J., 2012. The natural degradation of microcystins (cyanobacterial hepatotoxins) in fresh water - the future of modern treatment systems and water quality improvement. Pol. J. Environ. Stud. 21, 1125–1139.

Huang, L., Gan, L., Wang, N., Quan, X., Logan, B.E., Chen, G., 2012. Mineralization of pentachlorophenol with enhanced degradation and power generation from air cathode microbial fuel cells. Biotechnol. Bioeng. 109, 2211–2221.

Imanishi, S., Kato, H., Mizuno, M., Tsuji, K., Harada, K., 2005. Bacterial degradation of microcystins and nodularin. Chem. Res. Toxicol. 18, 591–598.

Ishii, H., Nishijima, M., Abe, T., 2004. Characterization of degradation process of cyanobacterial hepatotoxins by a gram-negative aerobic bacterium. Water Res. 38, 2667–2676.

Jung, S., Regan, J.M., 2007. Comparison of anode bacterial communities and performance in microbial fuel cells with different electron donors. Appl. Microbiol. Biotechnol. 77, 393–402.

Kato, H., Tsuji, K., Harada, K., 2009. Microbial degradation of cyclic peptides produced by bacteria. J. Antibiot. 62, 181–190.

Khan, M.I., Lee, M.G., Seo, H.J., Shin, J.H., Shin, T.S., Yoon, Y.H., et al., 2016. Enhancing the feasibility of Microcystis aeruginosa as a feedstock for bioethanol production under the influence of various factors. Biomed. Res. Int. 2016, 4540826.
Kohler, E., Villiger, J., Posch, T., Derlon, N., Shabarova, T., Morgenroth, E., et al., 2014. Biodegradation of microcystins during gravity-driven membrane (GDM) ultrafiltration. PLoS One 9, e111794.
Kormas, K.A., Lymperopoulou, D.S., 2013. Cyanobacterial toxin degrading bacteria: who are they? Biomed. Res. Int. 2013, 463894.
Kreetachat, T., Damrongsri, M., Punsuwon, V., Vaithanomsat, P., Chiemchaisri, C., Chomsurin, C., 2007. Effects of ozonation process on lignin-derived compounds in pulp and paper mill effluents. J. Hazard. Mater. 142, 250–257.
Kruger, T., Holzel, N., Luckas, B., 2012. Influence of cultivation parameters on growth and microcystin production of Microcystis aeruginosa (Cyanophyceae) isolated from Lake Chao (China). Microb. Ecol. 63, 199–209.
Kumar, G., Bakonyi, P., Kobayashi, T., Xu, K.Q., Sivagurunathan, P., Kim, S.H., et al., 2016. Enhancement of biofuel production via microbial augmentation: the case of dark fermentative hydrogen. Renew. Sust. Energ. Rev. 57.
Kumar, P., Hegde, K., Brar, S.K., Cledon, M., Kermanshahi-Pour, A., 2019. Potential of biological approaches for cyanotoxin removal from drinking water: a review. Ecotoxicol. Environ. Saf. 172, 488–503.
Logan, B.E., Hamelers, B., Rozendal, R., Schröder, U., Keller, J., Freguia, S., et al., 2006. Microbial fuel cells: methodology and technology†. Environ. Sci. Technol. 40, 5181–5192.
Luengo, E., Condón-Abanto, S., Álvarez, I., Raso, J., 2014. Effect of pulsed electric field treatments on permeabilization and extraction of pigments from Chlorella vulgaris. J. Membr. Biol. 247, 1269–1277.
Massey, I.Y., Yang, F., 2020. A mini review on microcystins and bacterial degradation. Toxins 12, 268.
Miguéns, D., Valério, E., 2015. The impact of some microcystins on the growth of heterotrophic bacteria from Portuguese freshwater reservoirs. Limnetica 34, 215–226.
Ndayisenga, F., Yu, Z., Yu, Y., Lay, C.H., Zhou, D., 2018. Bioelectricity generation using microalgal biomass as electron donor in a bio-anode microbial fuel cell. Bioresour. Technol. 270, 286–293.
Oh, H.-M., Lee, S.J., Jang, M.-H., Yoon, B.-D., 2000. Microcystin production by Microcystis aeruginosa in a phosphorus-limited chemostat. Appl. Environ. Microbiol. 66, 176–179.
Patil, S.A., Harnisch, F., Koch, C., Hübschmann, T., Müller, S., Kapadnis, B.P., 2016. Influence of pH on Formation, Performance, Electrochemical Characteristics and Composition of Bioelectrocatalytic Active Mixed Culture Biofilms in Bioelectrochemical Systems.
Pearson, L., Mihali, T., Moffitt, M., Kellmann, R., Neilan, B., 2010. On the chemistry, toxicology and genetics of the cyanobacterial toxins, microcystin, nodularin, saxitoxin and cylindrospermopsin. Mar. Drugs 8, 1650–1680.
Pham, T.H., Rabaey, K., Aelterman, P., Clauwaert, P., De Schamphelaire, L., Boon, N., et al., 2006. Microbial fuel cells in relation to conventional anaerobic digestion technology. Eng. Life Sci. 6, 285–292.
Ramani, A., Rein, K., Shetty, K.G., Jayachandran, K., 2012. Microbial degradation of microcystin in Florida's freshwaters. Biodegradation 23, 35–45.
Rastogi, R.P., Sinha, R.P., 2009. Biotechnological and industrial significance of cyanobacterial secondary metabolites. Biotechnol. Adv. 27, 521–539.
Reimers, C.E., Stecher III, H.A., Westall, J.C., Alleau, Y., Howell, K.A., Soule, L., et al., 2007. Substrate degradation kinetics, microbial diversity, and current efficiency of microbial fuel cells supplied with marine plankton. Appl. Environ. Microbiol. 73, 7029–7040.
Schmidt, J.R., Wilhelm, S.W., Boyer, G.L., 2014. The fate of microcystins in the environment and challenges for monitoring. Toxins 6, 3354–3387.
Smith, J.L., Boyer, G.L., Zimba, P.V., 2008. A review of cyanobacterial odorous and bioactive metabolites: impacts and management alternatives in aquaculture. Aquaculture 280, 5–20.
Speers, A.M., Reguera, G., 2012. Electron donors supporting growth and electroactivity of Geobacter sulfurreducens anode biofilms. Appl. Environ. Microbiol. 78, 437–444.
Tsao, S., Wei, D.-J., Chang, Y.-T., Lee, J.-F., 2017. Aerobic biodegradation of microcystin-LR by an indigenous bacterial mixed culture isolated in Taiwan. Int. Biodeterior. Biodegradation 124, 101–108.
Turula Jr, V.E., Gore, T., Singh, S., Arumugham, R.G., 2010. Automation of the anthrone assay for carbohydrate concentration determinations. Anal. Chem. 82 (5), 1786–1792. https://doi.org/10.1021/ac902664x.
Venkidusamy, K., Megharaj, M., 2016. Identification of electrode respiring, hydrocarbonoclastic bacterial strain Stenotrophomonas maltophilia MK2 highlights the untapped potential for environmental bioremediation. Front. Microbiol. 7, 1965.
Wu, Y., Arumugam, K., Tay, M.Q., Seshan, H., Mohanty, A., Cao, B., 2015. Comparative genome analysis reveals genetic adaptation to versatile environmental conditions and importance of biofilm lifestyle in Comamonas testosteroni. Appl. Microbiol. Biotechnol. 99, 3519–3532.
Xiong, H., Dong, S., Zhang, J., Zhou, D., Rittmann, B.E., 2018. Roles of an easily biodegradable co-substrate in enhancing tetracycline treatment in an intimately coupled photocatalytic-biological reactor. Water Res. 136, 75–83.
Yu, Y., Ndayisenga, F., Yu, Z., Zhao, M., Lay, C.-H., Zhou, D., 2019. Co-substrate strategy for improved power production and chlorophenol degradation in a microbial fuel cell. Int. J. Hydrog. Energy 44, 20312–20322.
Yuan, Y., Chen, Q., Zhou, S., Zhuang, L., Hu, P., 2011. Bioelectricity generation and microcystins removal in a blue-green algae powered microbial fuel cell. J. Hazard. Mater. 187, 591–595.
Zhang, C., Dong, S., Chen, C., Zhang, Q., Zhou, D., 2020. Co-substrate addition accelerated amoxicillin degradation and detoxification by up-regulating degradation related enzymes and promoting cell resistance. J. Hazard. Mater. 394, 122574.
Zhu, X., Yates, M.D., Logan, B.E., 2012. Set potential regulation reveals additional oxidation peaks of Geobacter sulfurreducens anodic biofilms. Electrochem. Commun. 22, 116–119.